Available online at www.sciencedirect.com
SCIENCE DIRECT®
C. R. Chimie 9 (2006) 702–707
COMPTES RENDUS CHIMIE
http://france.elsevier.com/direct/CRAS2C/

Preliminary communication / Communication

Chemical and electrochemical synthesis of nanosized TiO_2 anatase for large-area photon conversion

Babasaheb Raghunath Sankapal, Shrikrishna Dattatraya Sartale, Martha Christina Lux-Steiner, Ahmed Ennaoui *

Division of Solar Energy Research, Hahn-Meitner-Institut, Glienicker Strasse 100, 14109 Berlin, Germany

Received 3 July 2004; accepted after revision 16 June 2005

Available online 15 September 2005

Abstract

We report on the synthesis of nanocrystalline titanium dioxide thin films and powders by chemical and electrochemical deposition methods. Both methods are simple, inexpensive and suitable for large-scale production. Air-annealing of the films and powders at $T = 500$ °C leads to densely packed nanometer sized anatase TiO_2 particles. The obtained layers are characterized by different methods such as: X-ray diffraction (XRD), transmission electron microscopy (TEM), scanning electron microscopy (SEM), X-ray photoelectron spectroscopy (XPS) and atomic force microscopy (AFM). Titanium dioxide TiO_2 (anatase) phase with (101) preferred orientation has been obtained for the films deposited on glass; indium doped tin oxide (ITO) and quartz substrates. The powder obtained as the byproduct consists of TiO_2 with anatase-phase as well. ***To cite this article: B. R. Sankapal et al., C. R. Chimie 9 (2006)***.

Résumé

Nous rapportons sur la synthèse de couches minces et de poudre de dioxyde de titane TiO_2 nanocrystalline par des méthodes chimiques et électrochimiques. Les deux méthodes sont simples, peu coûteuses et bien adaptées pour des applications à grande échelle. Le recuit des films et des poudres à $T = 500$ °C permet d'obtenir des films denses et nanométriques de TiO_2 cristallisés dans la phase anatase. Les couches obtenues sont caractérisées par différentes méthodes : la diffraction des rayons X (XRD), la microscopie électronique en transmission (TEM), la microscopie électronique à balayage (SEM), la spectroscopie des photoélectron (XPS) et la microscopie à force atomiques (AFM). L'oxyde de titane TiO_2 (anatase) avec une orientation préférentielle (101) a été obtenue pour les films déposés sur le verre, l'oxyde d'étain et d'indium (ITO) et les substrats en quartz. La poudre obtenue comme sous-produit est aussi formée de nanoparticules de TiO_2 cristallisées dans la phase anatase. ***Pour citer cet article: B. R. Sankapal et al., C. R. Chimie 9 (2006)***.

Keywords: Chemical synthesis; TiO_2 (anatase); Thin films; Characterization

Mots-clés : Synthèse chimique ; TiO_2 anatase ; Couches minces ; Caractérisation

* Corresponding author.
E-mail address: ennaoui@hmi.de (A. Ennaoui).

1631-0748/$ - see front matter © 2005 Académie des sciences. Published by Elsevier SAS. All rights reserved.
doi:10.1016/j.crci.2005.06.035

1. Introduction

Titanium dioxide (TiO_2) is intensively studied because of its potential applications in various fields such as: liquid and solid nanostructured solar cells, with inorganic or organic extremely thin absorbers [1–4]. Furthermore, TiO_2 was investigated for catalysis and in electrochromic devices [5–7]. In the literature, several reports have recently appeared on TiO_2 thin films obtained by different techniques. Spray pyrolysis method has been employed to deposit TiO_2 thin film using titanium (IV) oxy-acetylacetonate 2-butanol solution with substrate temperature between 300 and 500 °C by Okuya et al. [8] and used for dye-sensitized solar cells. Karunagaran et al. [9] have used DC magnetron sputtering method to deposit TiO_2 films onto the Si-substrates and obtained mixture of anatase and rutile phases. Superionic cluster beams produced by pulsed micro-plasma cluster source have been used to prepare nanocrystalline thin films of TiO_2 by Taurino et al. [10]. Fang and Chen [11] used $TiCl_4$ in *n*-propanol to prepare Titania particles by thermal hydrolysis method. Spin-coating method has been used to deposit TiO_2 thin films using ammonium titanyl oxalate in aqueous solution [12]. Gao et al. [13] have used aqueous peroxotitanate solution at room temperature to deposit amorphous and nanometer sized TiO_2 thin films. Vigil et al. [14] have used microwave radiation heating to activate a flow of Titania precursor, which leads to the deposition of TiO_2 layers. Recently, Vigil et al. [15] have used microwave chemical bath deposition method for the deposition of TiO_2 thin films. Oekermann et al. [16] studied electron transport and back reaction with nanocrystalline TiO_2 films prepared by hydrothermal crystallization. Natarajan and Nagami [17] have reported cathodic electrodeposition of nanocrystalline TiO_2 thin films using Ti powder with H_2O_2 and ammonia. Karuppuchamy et al. [18] have modified this process. They used $TiOSO_4$ with H_2O_2 for the electrodeposition of TiO_2 thin films.

Due to the demands of TiO_2 in different applications, simple and low cost techniques are required for thin film deposition. Chemical and electrochemical methods are emerging as important *synthetic* methods to thin films not only for their cost effectiveness but also for the high quality of the materials. These methods are suitable for large area and even for complex structures. In the present investigation, we report on the chemical and electrochemical synthesis of nanocrystalline TiO_2 anatase thin films and powder. Characterizations were accomplished by using various techniques such as XRD, TEM, XPS, SEM, and AFM.

2. Experimental

All the chemicals are of highest purity (99.99%) and commercially available. They were used without further purification. Glass, commercially *available* indium tin oxide (ITO) coated glass (10 Ω/cm^2, Präzisions Glas and Optik GmbH, Germany) and quartz were used as substrates. Prior to the deposition the substrates were ultrasonically cleaned with acetone, ethanol and detergent and finally with ultra pure water.

2.1. Chemical synthesis

Aqueous solution was prepared by mixing 0.8 g of the titanium oxide sulfate ($TiOSO_4$) (Sigma-Aldrich Grade) and 2 ml H_2O_2 (30%) (Merck Grade) followed by 50 ml water in a beaker of capacity 100 ml. The obtained mixture was colloidal with pH ~2. The solution was initially orange/turbid and turned to clear red solution under constant stirring after 25 min at room temperature.

Deposition was carried out by vertical immersion of the substrates in the solution with continuous stirring. The substrates were withdrawn from the solution after certain deposition time (6 h for ITO and 12 h for films deposited on glass and quartz). After rinsing with distilled water, the samples were dried with nitrogen at room temperature (25 °C). The 'by-product' powder was collected through filtering, washed, dried, and submitted for further characterization

2.2. Electrochemical synthesis

The precursor bath consisted of 0.04 M $TiOSO_4$, 0.2 M H_2O_2 and 0.1 M KNO_3 (pH ~ 2) solutions maintained at room temperature (25 °C) was used for electrochemical synthesis. The clear solution was used as electrolyte. A conventional three electrodes electrochemical cell was used for electrosynthesis. Saturated calomel electrode (SCE) was used as reference and all the potentials were quoted with respect to this reference. The counter and working electrodes were pla-

tinium and ITO coated glass, respectively. The deposition was carried out by applying –1.2 V potential vs. SCE for 3 h. During deposition, the bath solution was continuously stirred. Typically 3 h deposition resulted in a smooth and flat film with a thickness of 50 nm. As a result of hydrolysis white amorphous titanium oxyhydroxide gel particles were observed in the bath after 3 h. The formed gel powder in the bath was collected by filtering the solution.

The films and the byproducts were annealed in air at 400, 450 and 500 °C temperatures. It was observed that annealing at 500 °C for 1 h had better cystallinity than others. Annealing treatment allowed converting the amorphous film into anatase-phase. The annealing temperature of 500 °C was chosen for further studies.

2.3. Characterizations

X-ray diffraction (XRD) spectra were recorded with an automated Bruker D8 advance X-ray diffractometer with the following characteristics: Cu Kα, $\lambda = 1.5406$ Å, 40 kV, 40 mA and $2\theta = 20$–$80°$. Measurements for thin films were taken using a glancing angle detector at $\theta = 1°$. Steps and collection time were, respectively, 0.01° and 7 s. The average crystallite size was determined with the Scherrer's method associated with the Topas 1.0 software. The phase composition was identified using the program EVA (version 4.0) provided by Bruker diffractometer.

Philips CM12 microscope operated at 120 kV was used for performing transmission electron microscopy (TEM). Axial illumination as well as the 'nanoprobe mode', with a beam spots size of 1.5 nm was used to identify diffraction of individual clusters. High-resolution (HRTEM) images were digitally recorded by using a CCD camera. XPS measurements were performed using a Leybold EA11 MCD spectrometer with an Mg Kα source at 1253.6 eV. The base pressure was 2×10^{-8} Pa. Peaks were fitted with Gauss–Lorentz shapes.

Scanning electron microscopy (SEM) images were recorded using a LEO1530 (Gemini) FE-SEM microscope with Schottky field emission and acceleration voltage of 10 kV. Atomic force microscopy (AFM) images were recorded using the Nanoscope IIIa scanning probe microscope in a contact mode. The commercial n^+-silicon cantilevers were used with a typical spring constant of 0.2 N/m in order to investigate the surface roughness.

3. Results and discussion

3.1. Structural studies

TiO_2 has three well-known phases namely: anatase, rutile, and brookite [5]. Rutile and anatase are tetragonal whereas brookite is orthorhombic. Rutile is the only stable phase. Anatase and brookite are metastable at all temperatures, and can be converted to rutile after heat treatment at high temperature. Fig. 1 shows XRD pattern of TiO_2 films deposited on ITO substrates by chemical (Fig. 1b) and electrochemical (Fig. 1c) method. ITO substrate was used as a reference (Fig. 1a). The most intense (101) peak of the TiO_2 in the X-ray pattern (Fig. 1b) for chemical deposited film was observed at $2\theta = 25.3°$ with a full width of 0.25° at a half-maximum intensity along with tiny peaks of (220) and (105) planes. This is an indication of interference-free reflection of the typical tetragonal-anatase as compared to standard JCPDS data [19]. Obviously XRD patterns do not shows any rutile or brookite peaks. Similar crystal structure was observed for electrodeposited films on ITO and chemically deposited films on glass and quartz substrates (see Fig. 2a, b). We observed that low deposition rate was favored for the films on glass and quartz substrates hence the deposition was performed for 12 h in order to get thicker films for structural analysis. Furthermore, the collected byproduct from chemical bath showed polycrystalline nature with

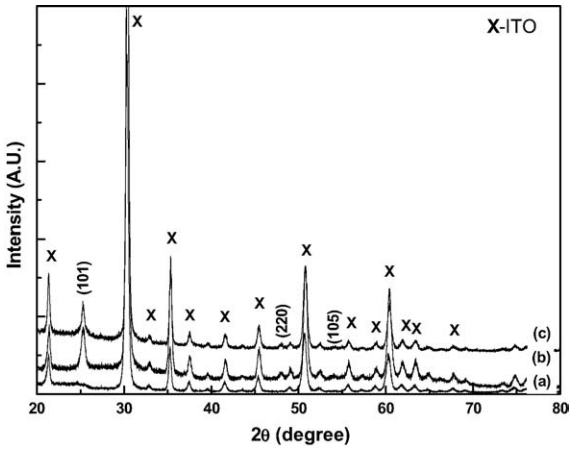

Fig. 1. X-ray diffraction patterns of (a) ITO (as reference) and TiO_2 films deposited by (b) chemical and (c) electrochemical methods on ITO substrate followed by annealing at 500 °C for 1 h in air.

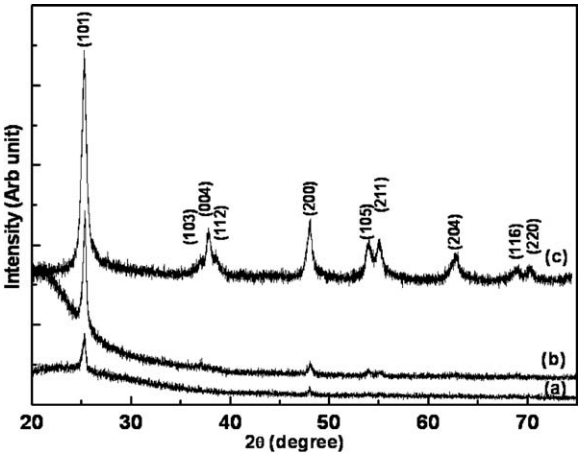

Fig. 2. X-ray diffraction patterns of chemically deposited TiO_2 thin films annealed at 500 °C for 1 h in air on (a) the glass substrate (b) the quartz substrate and (c) the collected byproduct annealed at 500 °C for 1 h in air.

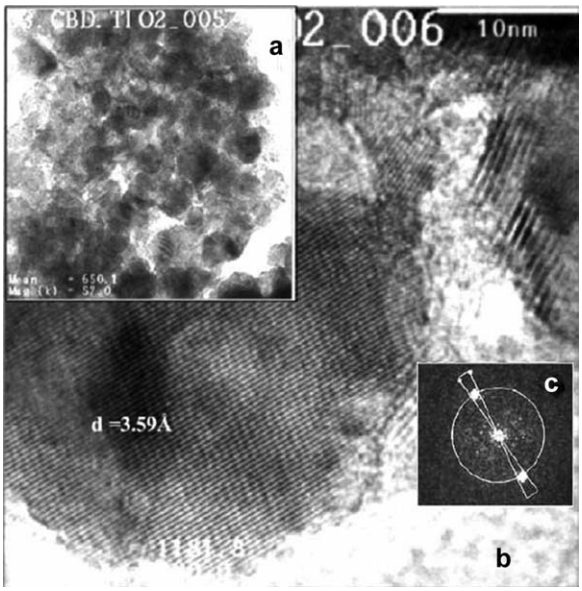

Fig. 3. (a) Inset shows TEM image of the TiO_2 film deposited by chemical method followed by annealing at 500 °C for 1 h in air. (b) A high-resolution image of a portion of the investigated image in (a). Results obtained after Fourier transformation of the high-resolution image is as shown in (c).

preferred orientation along (101) plane with anatase structure (see Fig. 2c). Using Scherrer's formula, we evaluated the crystallites size along (101) orientation. We obtained 16, 24 and 23 nm, respectively, for the films on ITO, glass, and quartz substrates, respectively, for chemically deposited films. The crystallite size for collected powder was 17 nm. Crystallite size of 23 nm was estimated for electrodeposited films.

Figs. 3 and 4a show transmission electron micrographs of the TiO_2 film deposited by chemical and electrochemical methods on glass and ITO substrates, respectively. The images exhibited a spherical and elongated shaped particles with roughly uniform in size of about 20–30 nm. High-resolution TEM images shows clearly developed lattice feature (Figs. 3 and 4b) which indicates that each of these larger particles is an agglomeration of smaller particles, with nanostructured domain. Fourier transformation (Figs. 3 and 4c) leads to demonstrate the inter-planer distance (*d*-spacing) of 3.59 and 3.45 Å for chemically and electrochemically deposited films, respectively. Comparing *d*-spacing with standard JCPDS data, we conclude that the anatase-phase with specific orientation along (101) direction was observed [19].

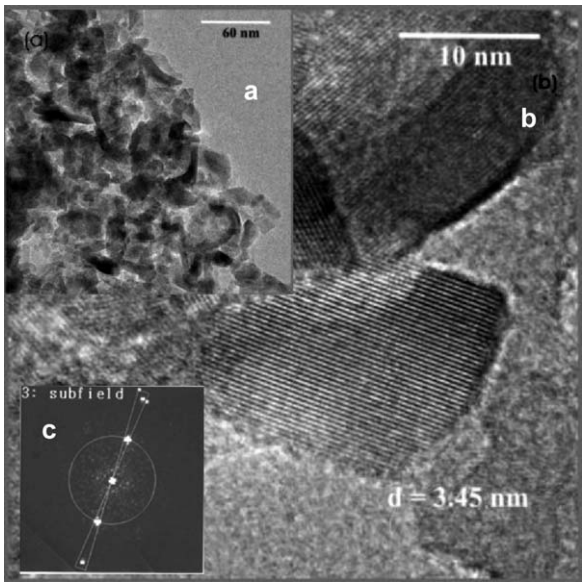

Fig. 4. (a) Inset shows TEM image of the TiO_2 film deposited by electrochemical method followed by annealing at 500 °C for 1 h in air. (b) A high-resolution image of a portion of the investigated image in (a). Results obtained after Fourier transformation of the high-resolution image is as shown in (c).

3.2. XPS measurements

XPS measurement was performed for chemically deposited films. Fig. 5a shows the XPS survey spectra

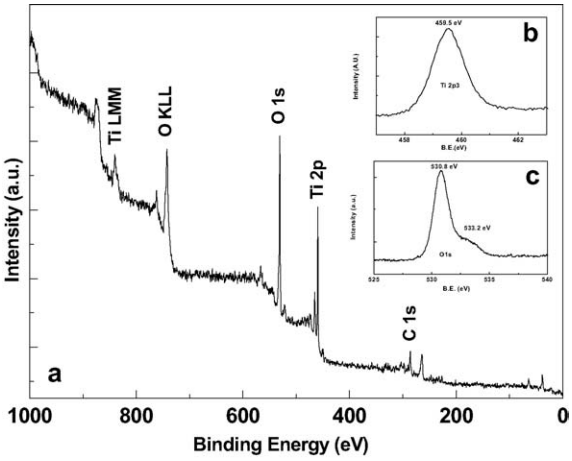

Fig. 5. (a) Elemental XPS spectra of the TiO_2 film by chemical method followed by annealing at 500 °C for 1 h in air. Insets (b) and (c) show high-resolution scans for Ti_{2p3} and O_{1s}, respectively.

of the TiO_2 film deposited on the ITO substrate. Major characteristic transition peaks for Ti, O and C are indicated. The $2p_{3/2}$ peak for Ti has a binding energy of 453.8 eV for metal, 455.1 for TiO, 458.5 for TiO_2 while 459.2 for anatase/rutile TiO_2 [20]. The high-resolution scan (inset in Fig. 5b) showed that the photoelectron peak for Ti at 459.5 eV, which is in the form of TiO_2, corresponds to anatase-phase, also supported by structural studies. In the present case, we observed that the O_{1s} peak was composed of two peaks revealing the presence of two forms of oxygen (inset Fig. 5c). The analysis by deconvolution shows two peaks at 530.8 and 533.2 eV. The major peak at 530.8 eV well matched with 530.1 eV for TiO_2 [20]. The minor peak might be due to the oxygen from the surface contamination, which is common for chemical deposited films. Also, some part of oxygen bonded with hydrogen cannot be excluded in the present case [20]. In addition to that, contamination of the surface by carbon is evident as peak for this element is already visible at 285.8 eV for the virgin TiO_2 surface [21].

3.3. Surface morphology

SEM images of TiO_2 on ITO substrate deposited by (a) chemical and (b) electrochemical methods are shown in Fig. 6. Small grains with dense structure and well surface coverage are observed for chemically deposited film. SEM cross-section of the TiO_2 film (see inset)

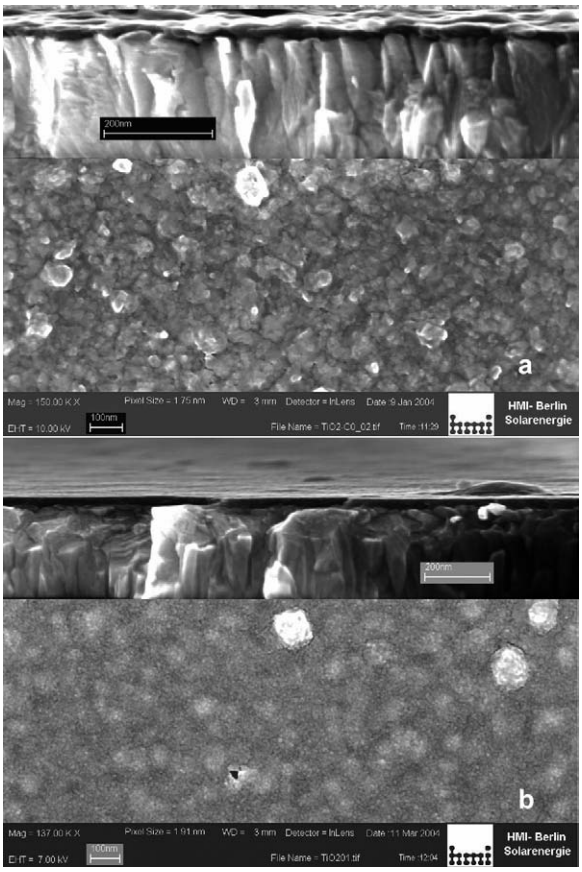

Fig. 6. SEM images of the TiO_2 films deposited by (a) chemical and (b) electrochemical methods followed by annealing at 500 °C for 1 h in air. Inset is the cross-section images, shows the compactness of the films.

shows compact film with a thickness around 20 nm. For electrochemically deposited films, a conformal coverage of the ITO substrate without any cracks or holes was obvious. The electrodeposited film is compact with a thickness of 50 nm as estimated by cross-sectional analysis (see inset).

AFM studies in contact mode were performed for TiO_2 film deposited by (a) chemical and (b) electrochemical methods on the ITO substrates (see Fig. 7). The films were dense and compact. Evaluation of surface patterns was conducted by estimating the roughness of the film (root-mean-squared). The root-mean-square (r.m.s.) roughnesses of 9 and 10 nm were evaluated from 9 μm^2 surface area for chemical and electrochemical deposited films, respectively.

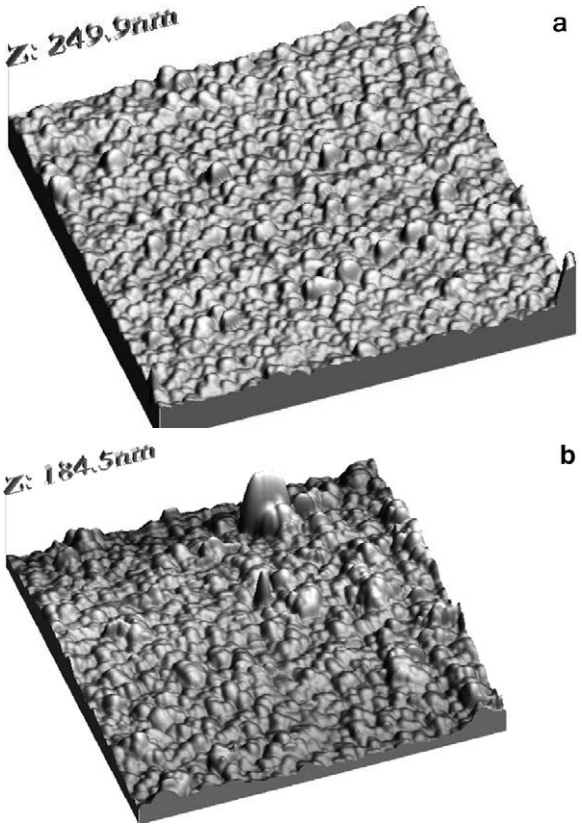

Fig. 7. Surface view AFM image of the TiO_2 films deposited by (a) chemical method and (b) electrochemical method followed by annealing at 500 °C for 1 h in air.

4. Conclusions

Chemical and electrochemical methods have been successfully used for the synthesis of TiO_2 thin films and powders as byproduct. Both chemical and electrochemical methods are simple and suitable for the preparation of large area TiO_2 anatase films by one step process. Air-annealing at 500 °C of as deposited amorphous films leads to the formation of anatase-phase. The annealed byproducts showed TiO_2 anatase structure as well. The dense, uniform and compact films on ITO substrates were observed by surface morphological studies. Nanocrystallites consisting of agglomerations of small particles are revealed by TEM and HRTEM analysis.

Acknowledgements

One of the authors S.D.S. acknowledges to Alexander von Humboldt (AvH), Foundation, Germany, for the financial support.

References

[1] B. O'Regan, M. Grätzel, Nature 353 (1991) 737.
[2] U. Bach, D. Lupo, P. Comte, J.E. Moser, F. Wiessörtel, J. Salbeck, H. Spreitzer, M. Grätzel, Nature 395 (1998) 583.
[3] M. Yeon Song, K.-J. Kim, D.Y. Kim, Solar Energy Mater. Solar Cells 85 (2005) 31.
[4] A. Belaidi, R. Bayón, L. Dloczik, K. Ernst, M.C. Lux-Steiner, R. Könenkamp, Thin Solid Films 431–432 (2003) 488.
[5] U. Dielbold, Surf. Sci. Rep. 48 (2003) 53.
[6] D.M. Blake, NREL/TP-570-26797 (1997) Report; www.osti.gov/brodge.
[7] H.A. Al-Abadleh, V.H. Grassian, Surf. Sci. Rep. 52 (2003) 63.
[8] M. Okuya, K. Nakade, S. Kaneko, Sol. Energy Mater. Sol. Cells 70 (2002) 425.
[9] B. Karunagaran, R.T.R. Kumar, V.S. Kumar, D. Mangalaraj, S.K. Narayandass, G.M. Rao, Mater. Sci. Semicond. Proc. 6 (5–6) (2003) 547.
[10] A.M. Taurino, S. Capone, P. Siciliano, T. Toccoli, A. Boschetti, L. Guerini, S. Iannotta, Sensors Actuators B92 (2003) 292.
[11] C. Fang, Y. Chen, Mater. Chem. Phys. 78 (2003) 739.
[12] K.R. Patil, S.D. Sathaye, Y.B. Khollam, S.B. Deshpande, N.R. Pawaskwar, A.B. Mandale, Mater. Lett. 57 (2003) 1775.
[13] Y. Gao, Y. Masuda, Z. Peng, T. Yonezawa, K. Koumoto, J. Mater. Chem. 13 (2003) 608.
[14] E. Vigil, J.A. Ayllon, A.M. Peiro, R. Roudriguez-Clemente, X. Domenech, J. Peral, Langmuir 17 (2001) 891.
[15] E. Vigil, B. Gonzalez, I. Zumeta, S. Docteur, A.M. Peiro, D. Gutierrez-Tauste, C. Dominogo, X. Domenech, J.A. Ayllon, J. Crystal Growth 262 (2004) 366.
[16] T. Oekermann, D. Zhang, T. Yoshida, H. Minoura, J. Phys. Chem. B 108 (2004) 2227.
[17] C. Natarajan, G. Nagami, J. Electrochem. Soc. 143 (1996) 1547.
[18] S. Karuppuchamy, K. Nonomura, T. Yoshida, T. Sugiura, H. Minoura, Solid-State Ionics 151 (2002) 19.
[19] JCPDS X-ray diffraction card no. 84-1285, 1994.
[20] J.F. Moulder, W.F. Stickle, P.E. Sobol, K.D. Bomben, in: J. Chastain (Ed.), Handbook of X-ray Photoelectron Spectroscopy, Perkin-Elmer Corp., USA, 1992.
[21] V.B. Gusev, L.M. Lenev, I.I. Kalinichenko, Zh. Prikl. Spektrosk. 34 (1981) 939.